Check for updates

View Article Online
View Journal

ChemComm

Accepted Manuscript

This article can be cited before page numbers have been issued, to do this please use: Y. Feng, X. Shao, K. Huang, J. Tian, X. Mei, Y. Luo and W. Xu, *Chem. Commun.*, 2018, DOI: 10.1039/C8CC03851A.

This is an Accepted Manuscript, which has been through the Royal Society of Chemistry peer review process and has been accepted for publication.

Accepted Manuscripts are published online shortly after acceptance, before technical editing, formatting and proof reading. Using this free service, authors can make their results available to the community, in citable form, before we publish the edited article. We will replace this Accepted Manuscript with the edited and formatted Advance Article as soon as it is available.

You can find more information about Accepted Manuscripts in the author guidelines.

Please note that technical editing may introduce minor changes to the text and/or graphics, which may alter content. The journal's standard Terms & Conditions and the ethical guidelines, outlined in our author and reviewer resource centre, still apply. In no event shall the Royal Society of Chemistry be held responsible for any errors or omissions in this Accepted Manuscript or any consequences arising from the use of any information it contains.

ROYAL SOCIETY OF CHEMISTRY

rsc.li/chemcomm

Please do not adjust margins

ROYAL SOCIETY OF CHEMISTRY View Article Online
DOI: 10.1039/C8CC03851A

Journal Name

COMMUNICATION

Mercury Nanoladders : A New Method for DNA Amplification, Signal Identification and Its Application on the Detection of Hg(II) Ions

Yuxiang Feng[*b], Xiangli Shao[*a,b], Kunlun Huang[a,b,c], Jingjing Tian[b], Xiaohong Mei[b], Yunbo Luo[a, **b], Wentao Xu[a, b, **c]

Received 00th January 20xx,
Accepted 00th January 20xx

DOI: 10.1039/x0xx00000x

www.rsc.org/

Published on 08 June 2018. Downloaded by Hacettepe Universitesi on 08/06/2018 16:35:07.

A biosensor based on Hg(II) nanoladders integrated with graphene oxide（GO） for Hg(II) detection was developed. Nanoladders were essentially DNA sandwich structure supported by T- Hg(II)-T and were used for Hg(II) trapping and signal translation. GO was used to differentiate the fluorescence generated by Hg(II) nanoladders from background signal.

Of all the heavy metals that contaminate the world's soil and water, divalent mercuric ion is one of the most dangerous. Inorganic mercury is released into the ecosystem through numerous anthropogenic and natural sources[1], and is subsequently converted into methylmercury through biomethylation by certain prokaryotes in aquatic sediments[2]. Methylmercury is neurotoxic and a known cause of mercury-related neurological diseases including prenatal brain damage, cognitive and motion disorders, vision and hearing loss, and even death[3, 4]. Therefore, the routine detection of Hg(II) ions is central to the environmental monitoring[5].

Growing concern over Hg(II) contamination in water and food supplies has created an urgent demand for ultrasensitive, rapid, and environmentally tolerant tracking of Hg(II) in aqueous media. Various detection methodologies have been proposed to monitor trace amounts of aqueous mercury ions. Current quantitative approaches to Hg(II) screening in aqueous solutions include AAS[6, 7], ICP-OES[8], GC[9]. etc. Although these methods are very sensitive and accurate, they tend to call for sophisticated apparatuses and cumbersome sample preparation processes. New molecular biology-based biosensors have become popular due to their relative simplicity and low cost. The fundamental principle of these biosensors is the conversion of signals. Hg(II) ion chemical signals, acting as signal inputs, may be converted into other outputs such as optical and electrical signals with the auxiliary of nucleic acids[10]. In addition to nucleic acids, alternative materials, such as small molecules[11],electrochemical[12, 13], gold nanoparticles[14] and protein enzyme[15, 16] have been proposed to achieve this conversion. Most molecular biology-based methods are limited, however, by the necessity for molecule modification or protein enzyme-dependent processes. As a result, there is still demand for a simple and straightforward approach to Hg(II) ion analysis. In this study, we developed a enzyme-free, constant temperature, fluorescent nucleic acid biosensor based on Hg(II) nanoladders integrated with graphene oxide (HNIG) for rapid, sensitive and selective detection of Hg(II) in aqueous solutions. Hg(II) nanoladders was firstly developed in this work to realize DNA amplification, signal identification and transformation. Hg(II)-specific thymine-thymine (T-T) base pair has been proven effective as a component of Hg(II) sensing platforms. Thus, we were inspired by this structure to develop the Hg(II) nanoladders for signal identification and transmission. Hg(II) nanoladders system contain two specially designed oligonucleotide probes, FAM-P1 and P2, which both include two T-rich domains spaced by Watson-Crick (W-C) base-pairing oligonucleotide sequence spacers. T-rich domains selectively capture Hg(II). The interactions between thymine and Hg(II) yields Hg(II) nanoladders, which are essentially nicked double helices of alternating copolymers. Each nanoladder consists of a long double strand and relatively short sticky ends[17, 18]. The difference of fluorescence generated by single stranded FAM-P1 and Hg(II) nanoladders can then be determined by graphene oxide(GO).

GO, an oxidized version of graphene, is widely regarded as a promising material in the nanoelectronics and nanocomposites

[a] Beijing Advanced Innovation Center for Food Nutrition and Human Health, College of Food Science & Nutritional Engineering, China Agricultural University, Beijing 100083, China
[b] Key Laboratory of Safety Assessment of Genetically Modified Organism (Food Safety), Ministry of Agriculture, P.R. China ）, Beijing, 100083, China
[c] Beijing Laboratory for Food Quality and Safety, College of Food Science and Nutritional Engineering, China Agricultural University, Beijing 100083, China
† Corresponding Authors
Email: **lyb@cau.edu.cn and **xuwentao@cau.edu.cn;
Tel/Fax: +86 010 62736479.
Electronic Supplementary Information (ESI) available: The tables of the DNA sequences and different Tris-HCl buffers used in this work, the experimental section of our work, as well as the analytical performance of our detection methods in real samples are listed in the supporting information. See DOI: 10.1039/x0xx00000x
. See DOI: 10.1039/x0xx00000x

ChemComm Accepted Manuscript

Please do not adjust margins

View Article Online
DOI: 10.1039/C8CC03951A

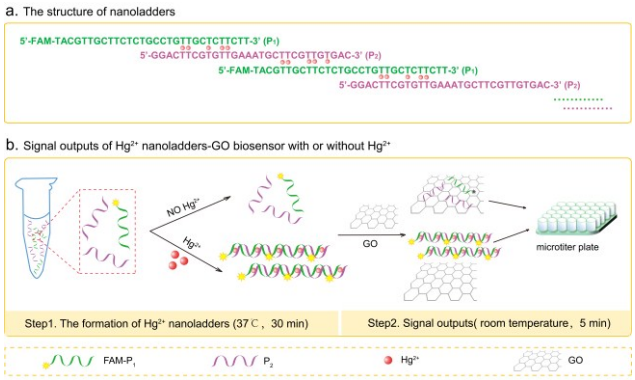

Scheme 1. Scheme of Hg(II) nanoladders and GO based HNIG biosensor for rapid detection of Hg(II) ions.a) Sequcences and basic structures of Hg(II) nanoladders; b) Different signal output in HNIG biosensoer with or without Hg(II) ions.

fields[19]. GO possesses distinct affinity characteristics for single-stranded DNA (ssDNA) and double-stranded DNA (dsDNA); ssDNA binds to GO with significantly higher affinity than dsDNA[20-22]. GO also has efficient quenching ability for ssDNA-labeled fluorochrome[23, 24]. In this study, Hg(II) nanoladders provide a strong fluorescence signal after GO was added, while the uncombined FAM-P1 and P2 are closely anchored onto the GO surface to reduce the background signal. To improve the signal-to-noise ratio, a DNA-GO interaction system was established after the concentration of probes and GO, ionic strength and solvent categories were optimized.

The diagram of the proposed HNIG-based detection system is provided in Scheme 1. The whole analysis procedure can be divided into three steps: triggering the the formation of Hg(II) nanoladders, GO adsorption and quenching, and the final fluorescent reading. In the first step, when Hg(II) was introduced into the system, thymine bases in FAM-P1 and P2 will interact with Hg(II) to form stable T-Hg(II)-T structures. Long double helices of Hg(II) nanoladders will be eventually yielded in this process. This cascade reaction will continue until the supply of the Hg(II) ions are exhausted. During the second step, due to the weak binding force between dsDNA and GO, Hg(II) nanoladders cannot be adsorbed on the GO surface, which lead to high fluorescence intensity. The fluorescence intensity driven by the nanoladders is then measured on a fluorescence spectrometer during the third step. On the contrary, in the absence of Hg(II), FAM-P1 and P2 coexist stably and remain single stranded, which will then be absorbed on the surface of GO. The fluorescence of FAM labeled on P1 is expected to be very weak due to the GO's superquenching capability.

The stability of Hg(II) nanoladders formed by different DNA were demonstrated by agarose gel electrophoresis (Support information, Figure S1). CD spectra of the nanoladders with or without Hg(II) were measured to examine the effects of Hg(II) ion binding on the higher-order structure of DNA. The CD spectra (Figure 1a) support the formation of the duplex structures in the presence of Hg(II), for the formation of T-

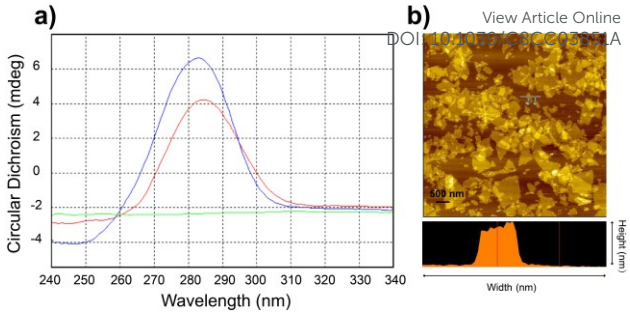

Figure 1. Structure of nanoladders and GO characterization. a) Secondary structure difference between nanoladders with or without Hg(II) was measured by CD. CD spectrum of P1+P2 in the absence (blue) and presence of Hg(II) (red), and Tris-HCl B1 buffer (green) were demonstrated. b) Tapping mode AFM images of GO.

Hg(II)-T structures within the DNA duplexes could cause a slightly red shift and a decrease value in the characteristic peaks[25]. This result indicates a significant change in the higher-order structure after addition of Hg(II) ions. The GO was characterized by AFM as shown in Figure 1b, the thickness of the GO sheets was around 1.60 nm, and it was confirmed that the GO was a monolayer and existed as exfoliated single sheets in solution. The sizes of the GO sheets ranged from nanometers to several micrometers.

The influence of different buffers on the HNIG biosensor was examined next. We tested PBS buffer, Tris-HCl buffer, HEPES buffer[26], and 4×SSC buffer in this experiment. The factor $(F_0\text{-}F)/F_0$ was defined as quenching efficiency to compare the performance of different buffers for Hg(II) analysis. F_0 and F represent the fluorescence intensity in the solution containing FAM-P1, P2(or T1), and GO in the absence and presence of target Hg(II) ions, respectively.

We first measured the $(F_0\text{-}F)/F_0$ values of FAM-P1+P2, FAM-P1+T1 and FAM-P1+P2+Hg(II) to verify the necessity of building

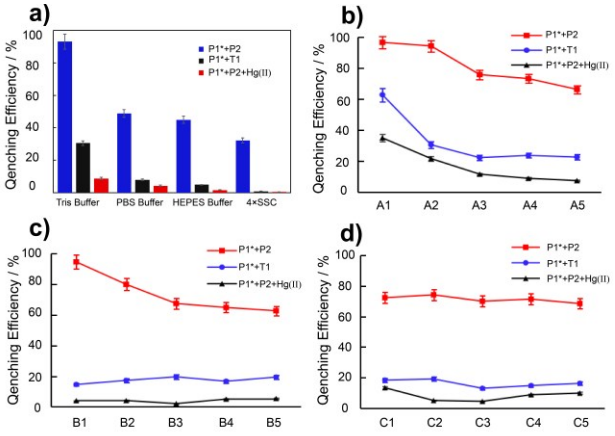

Figure 2. The $(F_0\text{-}F)/F_0$ values in different buffers. a) Quenching efficiency of four different buffers. And b), c), d) Quenching efficiency of Tris-HCl buffer with different components. The variable in each group were Tris, NaCl and $MgCl_2$,respectively.

Published on 08 June 2018. Downloaded by Hacettepe Universitesi on 08/06/2018 16:35:07.

ChemComm Accepted Manuscript

This journal is © The Royal Society of Chemistry 20xx

View Article Online
DOI: 10.1039/C8CC03851A

Published on 08 June 2018. Downloaded by Hacettepe Universitesi on 08/06/2018 16:35:07.

Hg(II) nanoladders. As illustrated in Figure 2a, the $(F_0\text{-}F)/F_0$ values of the sample containing FAM-P1 and P2 in Tris-HCl buffer was fairly high, with nearly 95% fluorescence quenching after the addition of GO in a DNA solution. By contrast, when FAM-P1 was hybridized with T1 to form a regular duplex, the FAM fluorescence was mostly retained in the presence of GO. However, the quenching efficiency of FAM-P1 and T1 was still twice as much as dsDNA built by the Hg(II) nanoladders. This observation demonstrated that the quenching efficiency was dependent on the length of the oligonucleotide: a longer sequence leads to lower quenching efficiency[20]. The high fluorescence quenching efficiency of FAM-P1+P2 and the distinguishable quenching characteristics between FAM-P1+T1 and Hg(II) nanoladders suggest that Tirs-HCl buffer was effective in Hg(II) detection.

We next sought to determine which component of the Tris-HCl buffer enhanced the quenching properties of GO and made the quenching efficiency of Hg(II) nanoladders and regular dsDNA distinguishable. The proportions of Tris, NaCl, and $MgCl_2$ were optimized. Buffers from A1 to C5 are listed on Table S2.

The relationship between the fluorescence quenching efficiency of GO and the components of Tris-HCl buffers is shown in Figure 2b-2d. At a low Tris level (0 mM and 1 mM), the regular dsDNA and Hg(II) nanoladders were not stable enough to keep away from the GO, thus a relatively high quenching efficiency was occured in dsDNA-GO system. Ionic strength, which was mainly influenced by the concentration of NaCl, had a significant effect on the quenching ability of GO as well. As shown in Figure 2c, lower ionic strength benefits the repulsion between Hg(II) nanoladders and GO while facilitate the attraction of ssDNA and GO. This occured due to the combined effect of both electrostatic repulsion and hydrophobic interactions[27]. The oxygen-containing functional groups dispersed on GO surface such as epoxide, hydroxyl and carboxylic acid groups were negatively charged in weak base solution[28]. Phosphate groups in dsDNA are polyanion, too. Therefore, dsDNA should be repelled by the negatively charged GO due to electrostatic repulsion in low ion intensity environment. However, aromatic and hydrophobic rings in both ssDNA bases and GO may attract each other through π-π stacking[29]. To facilitate these hydrophobic interactions, moderate cations are needed to screen the negative charge of phosphate and bring DNA close to the GO surface. Since divalent metal ions are much more effective in screening charges of two macromolecules, we selected buffer B1 as the optimal buffer per the results shown above.

The concentration of FAM-P1 should be controlled carefully to prevent increasing the signal-to-noise (SNR) ratio or decreasing the fluorescence intensity of the HNIG biosensor. To achieve rapid detection of Hg(II), an appropriate quenching time was also needed in our experiment. Thus, the fluorescence quenching kinetics in Tris-HCl buffer B1 was examined subsequently. The concentrations of FAM-P1 differed from 10 to 100 nM, while T1 and P2 was twice as much as FAM-P1 to

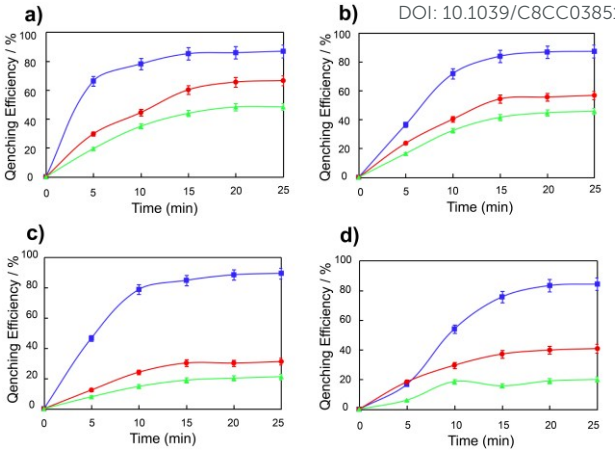

Figure 3. Effects of probes concentration on fluorescence response of the sensing system. Quenching efficiency of P1 and P2 in the absence (blue) and presence of 1μM Hg(II) (green), and complementary P1 and T1 (red) were demonstrated. The concentration of FAM-P1 was a)10 nM, b)20 nM, c)50 nM and d)100 nM, respectivly. The concentration of GO was 25μg/mL.

make sure the fluorescent probes were fully used. We also added 1 μM Hg(II) to the Hg(II) nanoladders system. As shown in Figure 3, the value of $(F_0\text{-}F)/F_0$ in all groups increased quickly as incubation time progressed until a steady state was reached after about 10 min. An ideal signal-to-noise ratio was achieved when the concentration of FAM-P1 was fixed in 50 nM. Therefore, 50 nM FAM-P1, and 100 nM P2 were used in all subsequent experiments.

The sensitivity and quantitative range of the HNIG biosensor were evaluated by detecting a series of different concentrations of Hg(II) under the optimal conditions we derived. Figure 4a shows the detection range of the HNIG sensing system upon GO addition after incubation with Hg(II) for 30 min. The fluorescence intensity increased with increasing Hg(II) concentration at any instantaneous time, and reached a plateau after 20 nM Hg(II) was added. As shown in Figure 4a (inset), the plot of fluorescence intensity versus the concentration of Hg(II)

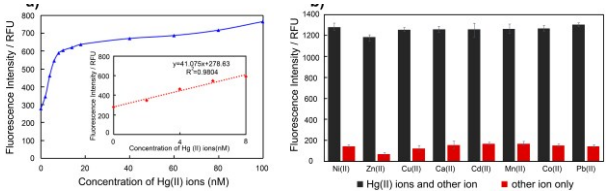

Figure 4. Hg(II) detection via HNIG biosensor.
a) Fluorescence response of HNIG sensing system at different Hg(II) concentrations. Inset: Linear relationship of HNIG biosensor with Hg(II) concentration ranged from 0 nM to 8 nM. b) Selectivity of the sensing method against other metal ions. Concentrations of Hg(II) and other metal ions were 1μM and 10 μM, respectively. All samples incubated for 30 min after 25 μg/mL GO was added.

ChemComm Accepted Manuscript

Published on 08 June 2018. Downloaded by Hacettepe Universitesi on 08/06/2018 16:35:07.

had a close linear relationship in the range from 0 to 8 nM with a regression equation expressed as y=41.075x+278.63 and correlation coefficient of R^2=0.9804. The sensitivity of our Hg(II) ion detection system was defined as the lowest concentration that could be stably detected, which we evaluated using serial dilutions of the 20 nM Hg(II) ion solution. We calculated the LOD as 1.5 nM per the rule of three times the standard deviation over the blank response[27].

The selectivity of HNIG system for Hg(II) detection was evaluated by monitoring the fluorescence response of the assay to other environmentally relevant divalent metal ions including Cd(II), Mn(II), Ca(II), Pb(II), Co(II), Cu(II), Zn(II), and Ni(II) at a concentration of 10 μM with or without 1μM Hg(II). As shown in Figure 4b, Hg(II) produced a significantly higher fluorescence signal compared to that of other metal ions. The coexistence of Hg(II) and other metal ions did not affect the detection sensitivity of the HNIG sensor. This is an essential requirement for practical applications because real samples typically contain different metal ions. The high selectivity of the sensing method is due to the fact that T-T mismatch shows high affinity for Hg(II) against many other metal ions.

To assess the feasibility of the HNIG biosensor for practical application, we conducted recovery experiments via standard addition method on drinking water samples. There was no Hg(II) presented in the water samples we collected, so we added additional Hg(II) manually to them for the purposes of the experiment.

The water samples were each gently mixed with Hg(II) standard solution to obtain two levels of final Hg(II) concentrations (3 nM and 6 nM). The results are summarized in Table S3. The proposed sensor indeed accurately measured the Hg(II) concentration in our drinking water samples.

In summary, we have developed a novel HNIG platform based on Hg(II) nanoladders and GO for the rapid analysis of Hg(II). Hg(II) nanoladders was served as a selective molecular recognition and signal transduction element, while GO was introduced into Hg(II) nanoladders system to build HNIG biosensors. Factors influence the detection effects of HNIG biosensor, including the adsorption buffer environment, final concentration of oligonucleotides in the Hg(II) nanoladders amplification volume and GO in HNIG system were carefully optimized. Under the optimal conditions, we measured LOD as low as 1.5 nM and the duration of the detection scheme was less than 40 min. Selectivity and practical detection tests returned stable quantitative results that were accurate for mixed substrates. We believe that the proposed HNIG sensor system accurately and efficiently detects mercury ions within different substrates.

Conflicts of interest

There are no conflicts to declare.

Notes and references

1. E. M. Nolan and S. J. Lippard, *Chemical reviews*, 2008, **108**, 3443-3480.
2. A. Ono and H. Togashi, *Angewandte Chemie International Edition*, 2004, **43**, 4300-4302.
3. P. M. Bolger and B. Schwetz, *New England Journal of Medicine*, 2002, **347**, 1735-1736.
4. G. Chen, Z. Guo, G. Zeng and L. Tang, *Analyst*, 2015, **140**, 5400-5443.
5. S. Yoon, A. E. Albers, A. P. Wong and C. J. Chang, *Journal of the American Chemical Society*, 2005, **127**, 16030-16031.
6. Y. Gao, Z. Shi, Z. Long, P. Wu, C. Zheng and X. Hou, *Microchemical Journal*, 2012, **103**, 1-14.
7. M. Ghaedi, M. Reza Fathi, A. Shokrollahi and F. Shajarat, *Analytical Letters*, 2006, **39**, 1171-1185.
8. N. H. Bings, A. Bogaerts and J. A. Broekaert, *Analytical chemistry*, 2006, **78**, 3917-3946.
9. W. F. Fitzgerald and G. A. Gill, *Analytical Chemistry*, 1979, **51**, 1714-1720.
10. P. Zhu, W. Tian, N. Cheng, K. Huang, Y. Luo and W. Xu, *Talanta*, 2016, **155**, 168-174.
11. E. Palomares, R. Vilar and J. R. Durrant, *Chemical Communications*, 2004, 362-363.
12. T. Yuan, Z. Liu, L. Hu, L. Zhang and G. Xu, *Chemical Communications*, 2011, **47**, 11951-11953.
13. A. Zahid, A. Lashin, U. A. Rana, N. Al-Arifi, I. Ullah, D. D. Dionysiou, R. Qureshi, A. Waseem, H.-B. Kraatz and A. Shah, *Electrochimica Acta*, 2016, **190**, 1007-1014.
14. J. S. Lee, M. S. Han and C. A. Mirkin, *Angewandte Chemie*, 2007, **119**, 4171-4174.
15. F. Xuan, X. Luo and I.-M. Hsing, *Analytical chemistry*, 2013, **85**, 4586-4593.
16. M. Yuan, Y. Zhu, X. Lou, C. Chen, G. Wei, M. Lan and J. Zhao, *Biosensors and Bioelectronics*, 2012, **31**, 330-336.
17. H. Torigoe, A. Ono and T. Kozasa, *Chemistry-A European Journal*, 2010, **16**, 13218-13225.
18. Z. Zhu, Y. Su, J. Li, D. Li, J. Zhang, S. Song, Y. Zhao, G. Li and C. Fan, *Analytical chemistry*, 2009, **81**, 7660-7666.
19. X. Deng, H. Tang and J. Jiang, *Analytical and bioanalytical chemistry*, 2014, **406**, 6903-6916.
20. S. He, B. Song, D. Li, C. Zhu, W. Qi, Y. Wen, L. Wang, S. Song, H. Fang and C. Fan, *Advanced Functional Materials*, 2010, **20**, 453-459.
21. L. Ge, W. Wang, X. Sun, T. Hou and F. Li, *Analytical chemistry*, 2016, **88**, 2212-2219.
22. L. Tang, H. Chang, Y. Liu and J. Li, *Advanced Functional Materials*, 2012, **22**, 3083-3088.
23. M. J. Allen, V. C. Tung and R. B. Kaner, *Chemical reviews*, 2009, **110**, 132-145.
24. H. Liu, L. Li, Q. Wang, L. Duan and B. Tang, *Analytical chemistry*, 2014, **86**, 5487-5493.
25. C.-W. Liu, Y.-T. Hsieh, C.-C. Huang, Z.-H. Lin and H.-T. Chang, *Chemical Communications*, 2008, 2242-2244.
26. J. R. Zhang, W. T. Huang, W. Y. Xie, T. Wen, H. Q. Luo and N. B. Li, *Analyst*, 2012, **137**, 3300-3305.
27. M. Wu, R. Kempaiah, P.-J. J. Huang, V. Maheshwari and J. Liu, *Langmuir*, 2011, **27**, 2731-2738.
28. Y. Wang, Z. Li, J. Wang, J. Li and Y. Lin, *Trends in biotechnology*, 2011, **29**, 205-212.
29. J. Antony and S. Grimme, *Physical Chemistry Chemical Physics*, 2008, **10**, 2722-2729.

View Article Online DOI: 10.1039/C8CC03851A

ChemComm Accepted Manuscript

This journal is © The Royal Society of Chemistry 20xx